

# FUNDAMENTALS OF TOMOGRAPHY AND RADAR

H.D. Griffiths and C.J. Baker  
*University College London*  
*UK*

**Abstract** Radar, and in particular imaging radar, has many and varied applications to security. Radar is a day/night all-weather sensor, and imaging radars carried by aircraft or satellites are routinely able to achieve high-resolution images of target scenes, and to detect and classify stationary and moving targets at operational ranges. Different frequency bands may be used, for example high frequencies (X-band) may be used to support high bandwidths to give high range resolution, while low frequencies (HF or VHF) are used for foliage penetration to detect targets hidden in forests, or for ground penetration to detect buried targets.

The techniques of tomographic imaging were originally developed in the context of medical imaging, and have been used with a number of different kinds of radiation, both electromagnetic and acoustic. The purpose of this presentation is to explore the application of tomographic imaging techniques at RF frequencies to a number of different applications in security, ranging from air defence to the detection of concealed weapons. Of particular interest is the use of ultra narrow band (UNB) transmissions with geometric diversity in a multistatic configuration to image moving targets. In the limit such transmissions could be CW, which would be particularly attractive for operation in a spectrally-congested environment. This arrangement effectively trades angular domain bandwidth for frequency domain bandwidth to achieve spatial resolution. Also of interest is the improvement in target classification performance afforded by multi-aspect imaging.

The presentation will review the theory of tomographic imaging, then discuss a range of applications to the overall security problem, the relevant system configurations in each case, the achievable performance and critical factors, and identify promising areas for future research.

**Keywords:**

radar; radar imaging; tomography; high resolution; synthetic aperture radar; interferometry; polarimetry; Radon transform; projection slice theorem; backprojection.

## 1. Introduction

Radar, and in particular imaging radar, has many and varied applications to security. Radar is a day/night all-weather sensor, and imaging radars carried by aircraft or satellites are routinely able to achieve high-resolution images of target scenes, and to detect and classify stationary and moving targets at operational ranges. Short-range radar techniques may be used to identify small targets, even buried in the ground or hidden behind building walls. Different frequency bands may be used, for example high frequencies (X-band) may be used to support high bandwidths to give high range resolution, while low frequencies (HF or VHF) are used for foliage penetration to detect targets hidden in forests, or for ground penetration to detect buried targets.

In the notes that follow we consider the formation of high-quality radar imagery, and the means by which it is possible to extract useful target information from such imagery.

## 2. Imaging and Resolution

Firstly we can establish some of the fundamental relations for the resolution of an imaging system. In the down-range dimension resolution  $\Delta r$  is related to the signal bandwidth  $B$ , thus

$$\Delta r = \frac{c}{2B}. \quad (1)$$

High resolution may be obtained either with a short-duration pulse or by a coded wide-bandwidth signal, such as a linear FM chirp or a step-frequency sequence, with the appropriate pulse compression processing. A short-duration pulse requires a high peak transmit power and instantaneously-broadband operation; these requirements can be relaxed in the case of pulse compression.

In the first instance cross-range resolution is determined by the product of the range and beamwidth  $\theta_B$ . The beamwidth is determined by the size of the aperture  $d$  and thus cross-range resolution is given by

$$\Delta x = r\theta_B \approx \frac{r\lambda}{d}. \quad (2)$$

As most antenna sizes are limited by practical aspects (such as fitting to an aircraft) the cross range resolution is invariably much inferior to that in the down range dimension. However, there are a number of techniques that can improve upon this. All of these are ultimately a function of the change in viewing or aspect angle. Thus in the azimuth (cross-range) dimension the resolution  $\Delta x$  is related to the change in aspect angle  $\Delta\theta$

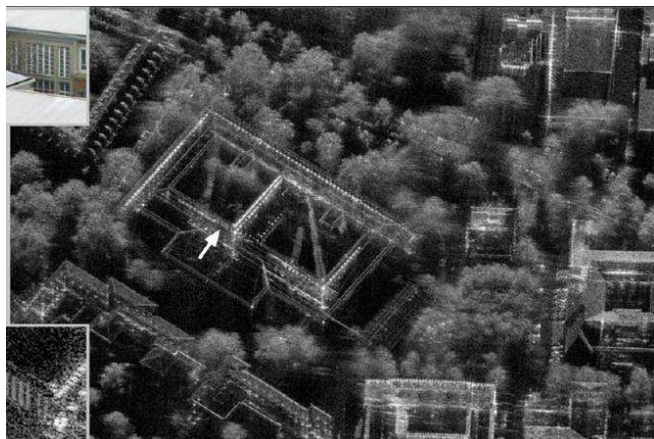


*Figure 1.* High resolution SAR image of a part of the university campus in Karlsruhe (Germany). The white arrow refers to a lattice in the left courtyard, which is shown in more detail in the small picture on the left bottom. The corresponding optical image is shown on the left top (after Brenner and Ender[4]).

as follows:

$$\Delta x = \frac{\lambda}{4 \sin\left(\frac{\Delta\theta}{2}\right)}. \quad (3)$$

For a linear, stripmap-mode synthetic aperture, equation (3) reduces to  $\Delta x = \frac{d}{2}$ , which is independent of both range and frequency. Even higher resolution can be obtained with a spotlight-mode synthetic aperture, steering the real-aperture beam to keep the target scene in view for a longer period, and hence forming a longer synthetic aperture.

Realistic limits to resolution may be derived by assuming a maximum fractional bandwidth  $\frac{B}{f_0}$  of 100%, and a maximum change in aspect angle of  $\Delta\theta = 30^\circ$  (higher values than these are possible, but at the expense of complications in hardware and processing). These lead to  $\Delta r = \Delta x = \frac{\lambda}{2}$ .

In the last year or so results have appeared in the open literature which approach this limit. Figures 1 and 2 show two examples from a recent conference of, respectively, an urban target scene and of aircraft targets. Critical to the ability to produce such imagery is the ability to characterise and compensate for motion errors of the platform, which can be done by autofocus processing [6]. Of course, motion compensation becomes most critical at the highest resolutions.

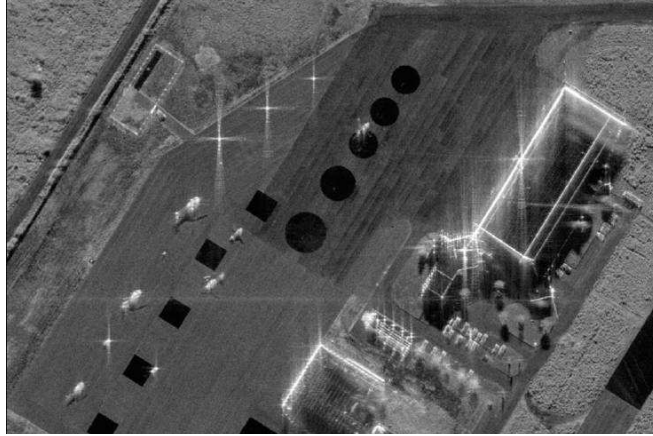


*Figure 2.* Example of 3-look image yielding 10 cm resolution (after Cantalloube and Dubois-Fernandez [5])

### 3. Tomographic Imaging

The techniques of tomography were developed originally for medical imaging, to provide 2D cross-sectional images of a 3D object from a set of narrow X-ray views of an object over the full  $360^\circ$  of direction. The results of the received signals measured from various angles are then integrated to form the image, by means of the Projection Slice Theorem. The Radon Transform is an equation derived from this theorem which is used by various techniques to generate tomographic images. Two examples of these techniques are Filtered Backprojection (FBP) and Time Domain Correlation (TDC). Further descriptions of these techniques may be found in [20].

In radar tomography the observation of an object from a single radar location can be mapped into Fourier space. Coherently integrating the mappings from multiple viewing angles enables a three dimensional projection in Fourier space. This enables a three dimensional image of an object to be constructed using conventional tomography techniques such as wavefront reconstruction theory and backprojection where the imaging parameters are determined by the occupancy in Fourier space. Complications can arise when target surfaces are hidden or masked at any stage in the detection process. This shows that intervisibility characteristics of the target scattering function are partly responsible for determining the imaging properties of moving target tomography. In other words, if a scatterer on an object is masked it cannot contribute to the imaging process and thus no resolution improvement is gained. However, if a higher number of viewing angles are employed then this

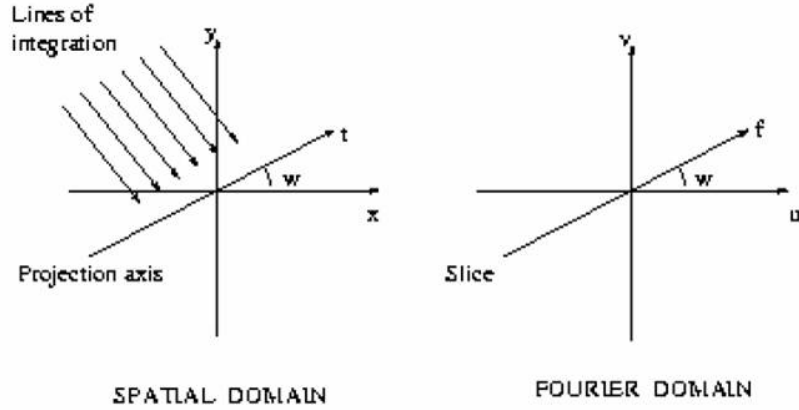


Figure 3. Tomographic reconstruction: the Projection Slice Theorem.

can be minimised. Further complications may arise if (a) the point scatterer assumption used is unrealistic (as in the case of large scatterers introducing translational motion effects), (b) the small angle imaging assumption does not apply and (c) targets with unknown motions (such as non-uniform rotational motions) create cross-product terms that cannot be resolved.

#### 4. The Projection Slice Theorem

The Tomographic Reconstruction (TR) algorithm makes use of the Projection-Slice theorem of the Fourier transform to compute the image. The Projection-Slice theorem states that the 1D Fourier transform of the projection of a 2D function  $g(x, y)$ , made at an angle  $w$ , is equal to a slice of the 2D Fourier transform of the function at an angle  $w$ , see Figure 3. Whereas some algorithms convert the outputs from many radars simultaneously into a reflectivity image using a 2D Fourier transform, TR generates an image by projecting the 1D Fourier transform of each radar projection individually back onto a 2D grid of image pixels. This operation gives rise to the term Backprojection. The image can be reconstructed from the projections using the Radon transform. The equation below shows this:

$$g(x, y) = \int_0^\pi \int_{-\infty}^{\infty} P(f) \cdot |f| \cdot e^{j2\pi f(x \cos w + y \sin w)} df dw \quad (4)$$

where  $w$  = projection angle

$P(f)$  = the Fourier transform of the 1-D projection  $p(t)$ .

The Filtered Backprojection (FBP) method may be used to process by reconstructing the original image from its projections in two steps: Filtering and Backprojection.

*Filtering the projection:* The first step of FB Preconstruction is to perform the frequency integration (the inner integration) of the above equation. This entails filtering each of the projections using a filter with frequency response of magnitude  $|f|$ .

The filtering operation may be implemented by ascertaining the filter impulse response required and then performing convolution or a FFT/IFFT combination to correlate  $p(t)$  against the impulse response.

*Backprojection:* The second step of FB Preconstruction is to perform the angle integration (the outer integration) of the above equation. This projects the 1D filtered projection  $p(t)$  onto the 2D image by following these steps: place a pixel-by-pixel rectangular grid over the XY plane, then place the 1D filtered projection  $p(t)$  in position at angle  $w$  for each pixel, then get the position of the sample needed from the projection angle and pixel position. Interpolate the filtered projection to obtain the sample. Add this backprojection value multiplied by the angle spacing. Repeat the whole process for each successive projection.

## 5. Tomography of Moving Targets

A development of these concepts has been the idea of imaging of moving targets using measurements from a series of multistatic CW or quasi-CW transmissions, giving rise to the term ‘ultra narrow band’ (UNB) radar. This may be attractive in situations of spectral congestion, in which the bandwidth necessary to achieve high resolution by conventional means (equation (1)) may not be available. Narrow band CW radar is also attractive as peak powers are reduced to a minimum, sidelobes are easier to control, noise is reduced and transmitters are generally low cost. Applications may range from surveillance of a wide region, to the detection of aircraft targets, to the detection of concealed weapons carried by moving persons. In general the target trajectory projection back to a given radar location will determine resolution. A random trajectory of constant velocity will typically generate differing resolutions in the three separate dimensions. However, even if there is no resolution improvement there will be an integration gain due to the time series of radar observations. A Hamming window or similar may be required to reduce any cross-range sidelobe distortions. The treatment which follows is taken from that of Bonneau, Bascom, Clancy and Wicks [3].

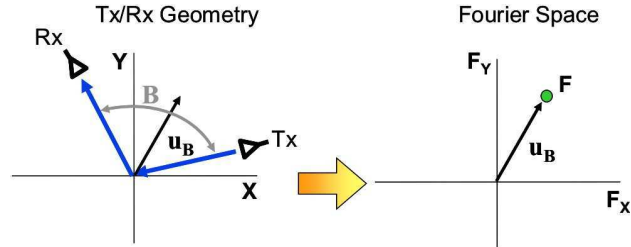


Figure 4. Relationship between bistatic sensor geometry and representation in Fourier space (after [3]).

Figure 4 shows the relationship between the bistatic sensor geometry and the representation in Fourier space. The bistatic angle is  $B$  and the bistatic bisector is the vector  $\mathbf{u}_B$ . The corresponding vector  $\mathbf{F}$  in

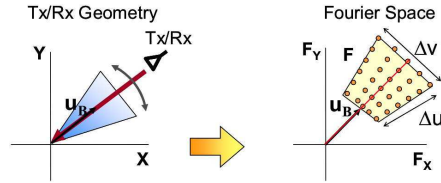


Figure 5. Fourier space sampling and scene resolution for a monostatic SAR (after [3]).

Fourier space is given by

$$\mathbf{F} = \frac{4\pi f}{c} \cos\left(\frac{B}{2}\right) \mathbf{u}_B \quad (5)$$

Figure 5 shows the equivalent relationship for a monostatic geometry. The resolutions are inversely proportional to the sampled extents  $\Delta u$  and  $\Delta v$  in Fourier space, thus

$$\Delta r = \frac{2\pi}{\Delta u} \quad \Delta x = \frac{2\pi}{\Delta v} \quad (6)$$

which should be compared to equations (1),(2) and (3).

In an UNB radar the finite bandwidth of the radar signal limits the range resolution. However, this resolution can be recovered by multi-static measurements over a range of angles. Figure 6 shows four examples, and the Fourier space sampling corresponding to each.

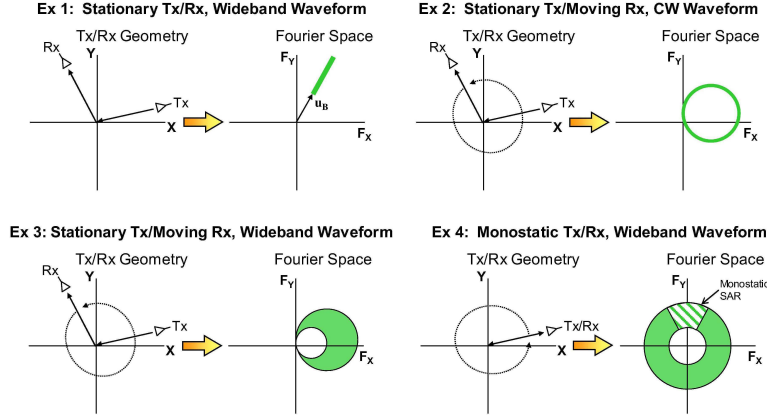


Figure 6. Fourier space sampling and scene resolution for four examples: (i) stationary tx/rx, wideband waveform; (ii) stationary tx, moving rx, CW waveform; (iii) stationary tx, moving rx, wideband waveform; (iv) monostatic tx/rx, wideband waveform (after [3]).

## 6. Applications

The applications of high resolution radar imagery are hugely varied and numerous. Invariably high resolution is used as a tool to improve the information quality resident in an electromagnetic backscattered signal. The resulting imagery may be used to gain information over extremely wide areas such as the earth's oceans, where data pertaining to sea state, current movements, etc. can be derived. Over the land, imagery is used for crop monitoring, evaluation of rain forest clearings, bio mass estimation and many other tasks. At the highest of resolution information on single objects is possible and it is here that the security applications are more likely. In particular improved detection and classification of objects such as vehicles, aircraft, ships and personnel, and at the very highest resolution, concealed weapons, are potentially possible. We consider a small sample here.

## 7. Automatic Target Recognition

These examples are illustrative of the potential of synthetic aperture imaging. However, it should be appreciated that the challenge is to extract useful information on the desired targets from such imagery.

The problem of determining the class to which a target belongs directly relies upon the amount of information available. ATRs are systems that contain an input sub-system that accepts pattern vectors from the

feature space, and a decision-maker sub-system that has the function of deciding the class to which the sensed attributes belong. Here we interchangeably refer to this process using the terms classification and recognition.

Pre-processing raw data is necessary in order to increase the quality of the radar signatures. Principal discriminating factors for classification purposes are Range Resolution, Side-Lobe Level (SLL) and Noise Level. Higher resolution means better point scatterers separation but the question of compromise regarding how much resolution is needed for good cost-recognition is difficult to resolve. Generally, high SLLs mean clearer range profiles but this also implies deterioration in resolution. Eventually, low noise levels mean high quality range profiles for classification. In this chapter we concentrate on the particular situation in which a single non-cooperative target has been previously detected and tracked by the system.

The improvement in performance due to the available multiplicity of perspectives is investigated examining one-dimensional signatures and the classification is performed on raw data with noise floor offset removed by target normalization. After generating a target mask in the range profile, the noise level is measured in the non-target zone and then subtracted from the same area. The result is a more prominent target signature in the range window.

Real ISAR turntable data have been used to produce HRR range profiles and images. In view of the fact that the range from the target is approximately constant, no alignment is needed. Three vehicle targets classified as A, B and C form the sub-population problem. Each class is described by a set of one-dimensional signatures covering 360 degrees of rotation on a turntable. After noise normalisation, a 28 dB SNR is achieved. Single chirp returns are compressed giving 30 cm of range resolution. The grazing angle of the radar is 8 degrees and 2'' of rotation is the angular interval between two consecutive range profiles. Therefore, 10000 range profiles are extracted from each data file over the complete rotation of 360 degrees. The training set of representative vectors for each class is made by 18 range profiles, taken approximately every 20 degrees for rotation of the target. The testing set of each class consists of the remaining range profiles excluding the templates.

Three algorithms have been implemented in both single and multi-perspective environments. In this way any bias introduced by a single algorithm should be removed. The first is the statistical Naïve Bayesian Classifier. It reduces the decision-making problem to simple calculations of feature probabilities. It is based on Bayes' theorem and calculates the posterior probability of classes conditioned on the given unknown feature

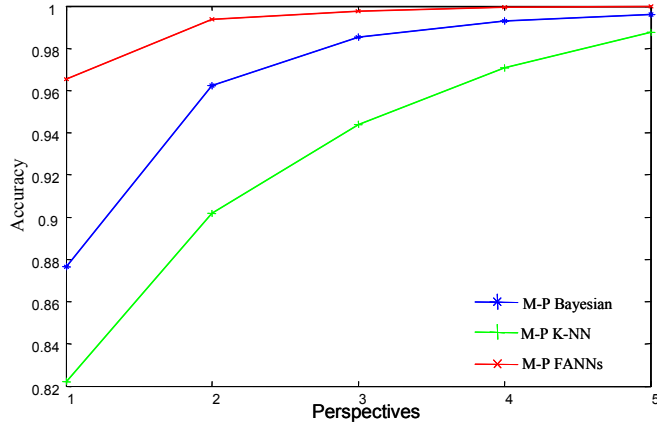


Figure 7. Multi-perspective classifier accuracies.

vector. The second is a rule-based method for classification: K-Nearest Neighbours (K-NN) algorithm. The rule consists of measuring and minimising the number of K distances from the object to the elements of the training set. The last approach involves Artificial Neural Networks (ANN), where the information contained in the training samples is used to set internal parameters of the network. In this work, Feed-forward ANNs (FANNs) supervised by a back-propagation strategy have been investigated and implemented.

We first consider classification based upon a multiplicity of viewing angles rather than using this multiplicity to form a single tomographic image. The combination of views of a target from a number of different aspects would be expected intuitively to provide an improvement in classification performance as clearly the information content should increase. Three different ways of combining the aspects are used here to illustrate possible performance improvements: These are the Naïve Bayesian Classifier, K-nearest neighbours (KNN), and Feed-forward Artificial Neural Networks (FANN). Details of these algorithms are provided in reference [21]. Figure 7 shows the improvement in classifier performance as a function of number of perspectives. In Figure 7, the classification performances of the three implemented classifiers are compared versus the number of perspectives used by the network. As anticipated, because of the nature of the data and the small available number of targets, the classifiers start from a high level of performance when using only a single aspect angle. It can be seen that there is a significant benefit in going from 1 to 2 perspectives, and a small additional benefit from 2 to 3, but rather less from further additional perspectives.

However, improved performance is achieved with increased radar number in the network. In particular, an improvement of 6.46% is shown comparing the single and the two-perspective classifier. The accuracy variation is then reduced to  $\pm 2.31\%$  overall for two to three perspectives,  $\pm 1.2\%$  for three to four and, finally,  $\pm 0.67\%$  for four to five perspectives. In conclusion, the greatest improvement in performance can be observed with just a small number of radars. Since the number of perspectives, and therefore the number of radars, is strictly related to complexity, costs and execution time of the network, for classification purposes it might be a reasonable trade-off implementing networks involving a small number of nodes. However this analysis is against a small number of target classes and these conclusions require further verification.

We now examine the extent to which SNR affects classification and whether multi-perspective scenarios are effective at different SNR levels. The FANNs classifier has been applied for this particular task. The range profiles are corrupted with additive white Gaussian noise. The original data, after noise removal, has a 28 dB SNR. Subsequently, the classifier is tested with range profiles with 24, 20 and 16 dB SNRs. The object has a length of 6.2 metres (it falls into about 20 range bins). As can be seen, as the SNR decreases, some of the useful features become less distinct, making the range profile more difficult to be classified. In Figure 8 performance is plotted versus the number of perspectives used and SNR levels, showing how the enhancement in classification varies with different noise levels. The plot shows an increase in classification performance with numbers of perspectives in each case. The increase is greater at the lowest values of SNR. However below an SNR of 15 dB the performance quickly degrades indicating that classifiers will be upset by relatively small amounts of noise.

## 8. Bandwidth Extrapolation

Radar resolution in range is directly limited by the bandwidth of the received signal (1). High resolution can thus be achieved by transmitting a wideband signal but at the expense of high spectrum occupancy. However, the actual trend is to favor more efficient use of the electromagnetic spectrum due to a growing need for commercial applications. In this context several solutions are proposed to create smarter transmitters and receivers. For instance, there is hope that cognitive radios could improve the RF spectrum occupancy in time by using devices that can “dynamically adjust their RF characteristics and performance in real time to reflect what may be a rapidly changing local interference environment” [24]. In radar, one solution consists of transmitting

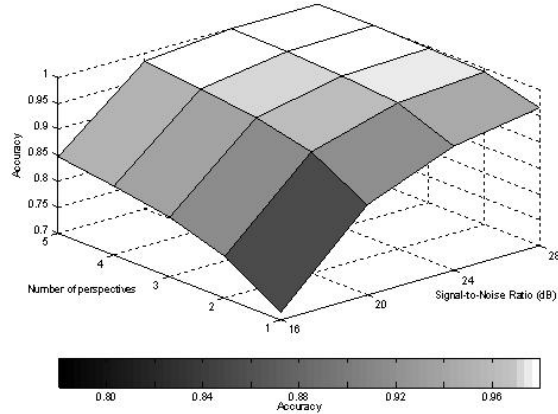


Figure 8. Variation with number of perspectives and signal-to-noise ratio.

narrow-band pulses and extrapolating the signal across a wider bandwidth. Bandwidth Extrapolation begins by fitting an *a priori* model to a measured radar signal. Auto-Regressive Models are commonly used for this purpose. These linear models are assumed to approximate scattering mechanisms that are often non-linear in practice. Model-parameter values can be obtained using super-resolution techniques such as MUSIC, Matrix Pencil and ESPRIT. Once the models have been fitted to the measured signal, they are utilised to predict the radar samples outside the band of measurements. Performances are affected in many ways by various parameters including Signal-to-Noise Ratio, target complexity and number of samples collected. In general, the models are deficient because part of the required information is corrupted by the noise. This particularly affects the extrapolation of a signal scattered by extended targets such as aircrafts [25]. Current research is focussed on the use of several bandwidths for building models that are more robust across a larger bandwidth. Such techniques can also be applied to ISAR image reconstruction when the initial signal is corrupted by interference.

In parallel with the development of bandwidth-extrapolation techniques is that of pattern recognition. Patterns created by the influence of the strongest scatterers on the target signature can be used to design additional knowledge-based methods. Patterns observed in time, frequency or angle provide information that can be used for classification and prediction. However, simple patterns are also associated with simple scattering mechanisms.

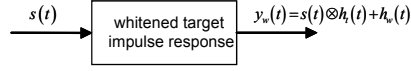


Figure 9. Whitening of the target impulse response in target-matched illumination.

## 9. Target-matched Illumination

The classical concept of the matched filter was further developed by Gjessing [9–11] and by Bell [2] to consider the optimum waveform for the detection of a target of a given range profile against a noise background. The target is characterized in terms of its impulse response as a function of delay time (i.e. range), which will also be a function of aspect angle (and therefore which in practice would require a library of target impulse responses versus aspect angle). The concept has been extended by Guerci, Pillai and co-workers [8, 13, 14, 19] to include the detection of a target against nonhomogeneous noise, and also to the problem of discriminating different targets. The problem is posed as follows (Figure 9) using the notation adopted by Guerci. The radar transmits a signal  $s(t)$  towards a target, whose impulse response is  $h_T(t)$ . The echo signal  $y(t)$  is the convolution of  $s(t)$  with  $h_T(t)$ . To this is added noise  $n(t)$ , so the received signal is

$$r(t) = (s(t) \otimes h_T(t)) + n(t) \quad (7)$$

where  $\otimes$  denotes the convolution operator.

The receiver is characterized by its impulse response  $h_R(t)$ . The problem is then to choose  $s(t)$  and  $h_R(t)$  to maximise the signal-to-interference ratio, which can be expressed in mathematical terms as follows:

$$y_0 = \max_s \max_h \rho(t_0) \quad (8)$$

where

$$SINR = \rho(t_0) = \frac{y_s^2(t_0)}{\langle y_0(t_0) \rangle^2}. \quad (9)$$

$y_s$  is the signal component of the output and  $y_0$  is the component contributed by interference and noise.

The first step is to maximise the SNIR working on the receiver. Once the optimal impulse response of the receiver,  $H_{MF}(t)$ , has been determined, it follows (Figure 9) that :

$$SNIR_0 \frac{1}{\sigma_w^2} \int_{T_i}^{T_f} |y_w(t)|^2 dt = f(s(t)) \quad (10)$$

where  $T_i$  and  $T_f$  are the time boundaries of the receiver and  $y_w(t)$  is the signal echo after the whitening filter.

At this stage, the problem is to maximise SNIR at the instant of detection  $t_0$  over the input signal  $s(t)$  of finite energy and duration. Grouping the expressions for both whitening filter and matched filter:

$$h(t) = h_T \otimes h_w(t). \quad (11)$$

Using this, the integral in (10) can be written

$$\int_{T_i}^{T_f} |y_w(t)|^2 dt = \int_0^T s(\tau_1) \cdot \int_0^T s^*(\tau_2) K^*(\tau_1, \tau_2) d\tau_2 d\tau_1 \quad (12)$$

where

$$K(\tau_1, \tau_2) = \int_{T_i}^{T_f} h^*(t - \tau_1) h(t - \tau_2) dt. \quad (13)$$

The solution must satisfy a homogeneous Fredholm integral of the second kind with Hermitian kernel:

$$\lambda_{\max} S_{opt}(t) = \int_0^T S_{opt}(\tau) K(t - \tau) d\tau. \quad (14)$$

This principle can be extended to different models including signal dependent noise (clutter) [19]. In this case, one must take the non-linear term into account in the signal to interference plus noise equation:

$$SINR_0 = \frac{\left| \frac{1}{2\pi} \int_{-\infty}^{+\infty} H_R(\omega) H_T(\omega) S(\omega) e^{-j\omega T_f} d\omega \right|^2}{\frac{1}{2\pi} \int_{-\infty}^{+\infty} |H_R(\omega)|^2 \cdot \left( G_n(\omega) + G_c(\omega) |S(\omega)|^2 \right) d\omega} \quad (15)$$

where

$G_n(\omega)$  is the additive noise spectrum,

$G_c(\omega)$  is the clutter spectrum,

$H_T(\omega)$  and  $H_R(\omega)$  are the transmitter and receiver spectrum respectively.

From the above model we can derive three main cases:

- a) the clutter is not significant compared to the additive noise:  
 $G_c(\omega) \ll G_n(\omega)$
- b) the additive noise is not significant relative to the clutter:  
 $G_c(\omega) \gg G_n(\omega)$

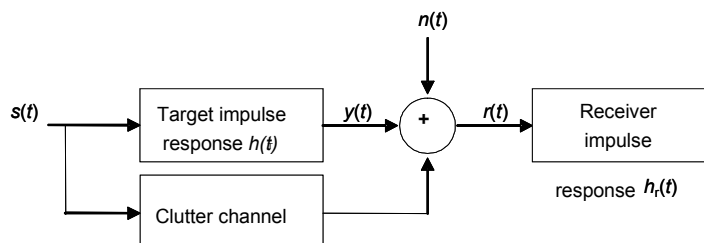


Figure 10. Target-matched illumination with signal-dependent noise (clutter).

c) clutter and noise are of equivalent power:

$$G_c(\omega) \sim G_n(\omega)$$

Unlike the first two cases, which can be solved by the previous method, the third one (clutter and noise) has been studied by Guerci using an iterative procedure [19].

*Applications:* Potential applications of matched illumination are:

- identical target resolution (Figure 10)
- target identification
- target tracking/tagging
- target aspect uncertainty.

## 10. Conclusion

The techniques described and the results presented demonstrate the value of radar imaging to security problems. In particular a novel multi-perspective approach to classification has been presented. High resolution data from turntable measurements have been processed and HRR range profiles and ISAR imagery from a number of radar targets have been successfully formed. Three algorithms for classification have been implemented using the radar signatures as the basis for recognition in both single and multi-perspective environments. Improvements in classification performance have been shown by using different information gathered by a network of radars whose nodes are placed around the target. In addition, the increase in recognition accuracy is not linear with the number of perspectives used. Greater positive variations can be seen for a small number of nodes employed in the network. Furthermore, the results obtained at lower SNR levels show valuable improvements in target recognition for more practical classification purposes. Alternatively the embedded information approach of target adaptive matched

illumination offers a means of directly implementing classification via exploitation of prior knowledge. Whilst encouraging, these conclusions should be treated with some caution as they are somewhat limited by the restricted available data.

## 11. Acknowledgements

We express our thanks to the students with whom we have worked on these subjects and whose results we have used, in particular Hervé Borrión, Shirley Coetzee and Michele Vespe, and to the organisations, including the UK Ministry of Defence, the US Air Force Office of Scientific Research, the UK Engineering and Physical Sciences Research Council, QinetiQ and its predecessors, BAE SYSTEMS, Thales Sensors and AMS, who have supported the various projects. We also thank Erik De Witte and Hervé Borrión for their help in rendering this document into L<sup>A</sup>T<sub>E</sub>X.

## References

- [1] Ausherman, D.A., Kozma, A., Walker, J.L., Jones, H.M. and Poggio, E.C., ‘Developments in radar imaging’, IEEE Trans. Aerospace & Electronics Systems, Vol. AES-20, pp 363-400, 1984.
- [2] Bell, M., ‘Information theory and radar waveform design’, IEEE Trans. Information Theory, Vol.39, No.5, pp 1578-1597, 1993.
- [3] Bonneau, R.J., Bascom, H.F., Clancy, J.T. and Wicks, M.C., ‘Tomography of moving targets (TMT)’.
- [4] Brenner, A.R. and Ender, J.H.G., ‘Airborne SAR imaging with subdecimetre resolution’, Proc. EUSAR 2004 Conference, pp 267-270.
- [5] Cantalloube, H. and Dubois-Fernandez, P. ‘Airborne X-band SAR imaging with 10 cm resolution—technical challenge and preliminary results’, Proc. EUSAR 2004 Conference, pp 271-274.
- [6] Carrara, W.G., Goodman, R.S. and Majewski, R.M., Spotlight Synthetic Aperture Radar: Signal Processing Algorithms, Artech House, 1995.
- [7] Coetzee, S.L., ‘Radar tomography of moving targets’, MPhil. Transfer thesis, University College London, 2004.
- [8] Garren, D.A., Osborn, M.K., Odom, A.C., Goldstein, J.S., Pillai, S.U. and Guerci, J.R., ‘Enhanced target detection and identification via optimized radar transmission pulse shape’, IEE Proc. Radar, Sonar and Navigation, Vol.148, No.3, pp 130-138, June 2001.
- [9] Gjessing, D.T., ‘Adaptive techniques for radar detection and identification of objects in an ocean environment’, IEEE J. Ocean Engineering, Vol.6, No.1, pp 5-17, 1981.
- [10] Gjessing, D.T., Target Adaptive Matched Illumination Radar: Principles and Applications, Peter Peregrinus, 1986.

- [11] Gjessing, D.T. and Saebboe, J., 'Bistatic matched illumination radar involving synthetic aperture and synthetic pulse for signal to clutter enhancement and target characterization', Proc. 2001 CIE International Conference on Radar, Beijing, pp 20-24, 15-18 October 2001.
- [12] Gjessing, D.T. and Saebboe, J., 'Bistatic matched illumination radar involving synthetic aperture and synthetic pulse for signal to clutter enhancement and target characterization', Proc. 2001 CIE International Conference on Radar, Beijing, pp 20-24, 15-18 October 2001.
- [13] Grieve, P.G. and Guerci, J.R., 'Optimum matched illumination-reception radar', US Patent S517522, 1992.
- [14] Guerci, J.R., 'Optimum matched illumination-reception radar for target classification', US Patent S5381154, 1995.
- [15] Knaell, K.K. and Cardillo, G.P., 'Radar tomography for the generation of three-dimensional images', IEE Proc. Radar Sonar Navig., vol. 142, no. 2, pp. 54-60, 1995.
- [16] Munson, D.C. Jr., O'Brien, J.D. and Jenkins, W.K., 'A tomographic formulation of spotlight-mode synthetic aperture radar', Proc. IEEE, Vol.71, No.8, pp 917-925, 1983.
- [17] Oliver, C.J. and Quegan, S., Understanding SAR Images, Artech House, 1998.
- [18] Pasmurov, A. Ya. and Zinoviev, Yu. S., Radar Imaging and Tomography, to be published by Peter Peregrinus, Stevenage, 2005.
- [19] Pillai, S.U., Oh, H.S., Youla, D.C. and Guerci, J.R., 'Optimum transmit-receiver design in the presence of signal-dependent interference and channel noise', IEEE Trans. Information Theory, Vol.46, No.2, pp 577-584, March 2000.
- [20] Soumekh, M., Synthetic Aperture Radar Signal Processing with MatLab Algorithms, Artech House, 1999.
- [21] Vespe, M., Baker, C.J. and Griffiths, H.D., 'Multi-perspective target classification', Proc. RADAR 2005 Conference, Washington DC, IEEE Publ. No. 05CH37628, pp 877-882, 9-12 May 2005.
- [22] Walker, J.L., 'Range Doppler imaging of rotating objects', IEEE Trans. AES, Vol. 16, pp 23-52, 1980.
- [23] Wehner, D.R., High Resolution Radar, Artech House, 1987.
- [24] Walko, J., 'Cognitive Radio', IEE Review, p36, May 2005.
- [25] Borrión, H., Griffiths, H. Money, D., Tait P. and Baker C., 'Scattering centre extraction for Extended targets', Proc. RADAR 2005 Conference, Washington DC, IEEE Publ., pp 173-178, 9-12 May 2005.